Formation of η-mesic Nuclei Using the Recoilless (d,^{3}He) Reaction

R.S. Hayano [a] S. Hirenzaki [b] and A. Gillitzer [c]

[a] *Department of Physics, University of Tokyo, Hongo, Bunkyo-ku, Tokyo 113, Japan*

[b] *Department of Physics, Nara Women's University, Nara 630, Japan*

[c] *Physik Department E12, Technische Universität München, D-85748 Garching, Germany*

Abstract

We propose to use the recoilless (d,^{3}He) reaction to produce η-mesic nuclei. This reaction has been used to observe deeply bound pionic states and proven to be powerful recently. We calculate η-mesic bound states in the nucleus using an optical potential and their formation cross section with the Green function method. Then, we carefully check the experimental feasibility. We find that η-mesic nuclei can be observed experimentally using the (d,^{3}He) reaction. We also mention the possibility to study the formation of ω-mesic nuclei.

Key words: (d,^{3}He) reaction, η-mesic nuclei
PACS: 25.10.+s; 14.40.Aq; 36.10.Gv

Bound states of η mesons in nuclei (η-mesic nuclei) are interesting objects which have not been observed so far experimentally. The η-meson is a member of the SU(3) nonet of pseudoscalar mesons and believed to be one of the Nambu-Goldstone bosons of spontaneous chiral symmetry breaking. The origin of the mass of the Nambu-Goldstone bosons is studied theoretically in terms of a symmetry breaking pattern[1]. Since chiral symmetry is expected to be partially restored at finite density[2], it is very interesting to study the behavior of mesons, especially their masses, in the nucleus.

Since the η-nucleon scattering length is dominated by the s-wave part due to the strong coupling to the $N^*(1535)$ resonance, the η-nucleus optical potential has a large s-wave part. Thus by spectroscopic studies of η-mesic nuclei, we can expect to obtain precise information on the s-wave potential, which is equivalent to the mass shift of the η-meson in the nucleus. We also expect to

get new information on the properties of the $N^*(1535)$ resonance in nuclear matter by studying the η-nucleus optical potential.

The in-medium behavior of π and K mesons, which are also Nambu-Goldstone bosons, has been reasonably well understood from scattering as well as mesic atom data. In contrast, there is little experimental information on the in-medium properties of the η meson. Existence of η-mesic nuclei was suggested theoretically by Haider and Liu[3]. They systematically investigated η-mesic nuclear states and proposed to use the (π^+, p) reaction for their formation. Experimental attempts to find a bound state in this reaction led to negative results[4]. On the other hand, the cross section for η meson production in d(p,^{3}He)η reactions at threshold was found to be large[5] and was analyzed in terms of a quasi-bound $\eta-{}^3$He system[6]. For the $\eta-{}^4$He system also the existence of a quasi-bound state was suggested[7]. Recent theoretical work indicated the existence of η-mesic nuclei, however their structure is only predicted with large uncertainty [8,9]. With the present knowledge, the existence of η-mesic nuclei is still controversial.

In this paper we discuss as a new experimental method to produce η-mesic nuclei in (d,^{3}He) transfer reactions on light target nuclei, as recently proposed at the GSI heavy-ion synchrotron SIS [10]. The (d,^{3}He) reaction at recoilless kinematics was proven to be a powerful experimental tool by the discovery of deeply bound pionic atom formation[11,12] and to be very useful to extract the pion properties at finite density[13,14]. Here we calculate the structure and formation cross section of η-mesic nuclear states theoretically and investigate the experimental feasibility. We should mention here that the same experimental technique can be used to produce other mesic nuclei. The ω meson is expected to be around 16% lighter at normal nuclear density than in free space[15] and expected to form quasi-bound states. The ω-mesic nuclear states can also be observed by the (d,^{3}He) reaction in principle as discussed in Ref. [10].

In order to study the structure of $\eta-$mesic nuclei, we used the first-order in density η-nucleus optical potential,

$$V_\eta = -\frac{4\pi}{2\mu}\left(1+\frac{m_\eta}{M_N}\right)a_{\eta N}\rho(r), \tag{1}$$

where $a_{\eta N}$ is the $\eta-$nucleon scattering length, μ is the reduced mass of the η and is $\sim m_\eta$ for heavy nuclei, M_N is the nucleon mass, and ρ is the nuclear density.

There exist several recent estimates on the ηN scattering length:

$$\begin{aligned} a_{\eta N} &= [(0.717 \pm 0.030) + i(0.263 \pm 0.025)]\mathrm{fm} \quad [16], && (2)\\ &= [(0.751 \pm 0.043) + i(0.274 \pm 0.028)]\mathrm{fm} \quad [17], && (3)\end{aligned}$$

$$\approx (0.52 + i0.25)\text{fm} \quad [7], \tag{4}$$
$$\approx (0.20 + i0.26)\text{fm} \quad [18]. \tag{5}$$

As shown, the first two theoretical estimates agree fairly well with each other. The third value was deduced from an experimental study of d(p,^{3} He)η and d(d,^{4} He)η reactions[7]. In all cases, the η-nucleus optical potential is expected to be attractive. For an illustrative purpose, let us take $\mu = m_\eta = 547$ MeV, $M_N = 939$MeV and $\rho_0 = 0.17\text{fm}^{-3}$ and $a_{\eta N} = 0.717 + 0.263\ i$fm. We then obtain

$$V(r) = -(86 + 32i)\rho(r)/\rho_0 \text{ MeV},$$

which is indeed strongly attractive. The imaginary part $W = -\Gamma/2$ is appreciable, but small enough compared with the real part.

With this potential, we calculated the η-nucleus binding energies and widths for various nuclei in a conventional way of solving the Klein-Gordon equation. The vector part of the potential, which in general must be taken into account, was ignored in these and the following calculations, based on the assumption that the $\eta - N$ interaction is dominated by the $s-$wave component. A Woods-Saxon form of the nuclear density profile was used, where nuclear radii and diffuseness were taken to be $R = 1.18A^{1/3} - 0.48$ fm and $a = 0.5$ fm, respectively. The results are shown in Table 1 for the case of $a_{\eta N} = (0.717 + 0.263i)$ fm and in Table 2 for the case of $a_{\eta N} = (0.20 + 0.26i)$ fm. We find that in the former case the half widths are comparable or smaller than the binding energies and/or level spacings, so that it is justified to interpret these states as quasi-stable $\eta-$mesic nuclear bound states.

Similar to the case of deeply-bound pionic atom production, it is possible to produce $\eta-$mesic nuclei near the recoilless condition using the (d,^{3}He) reaction on nuclear targets. This is illustrated in Fig. 1, which shows the momentum transfer q vs. the incident deuteron kinetic energy T_d for a typical light target nucleus (^{7}Li in this case). The use of recoilless kinematics is essential to suppress the quasi-free continuum η production and to enhance the $\eta-$mesic nuclear production signal. The recoil-free η condition is satisfied at $T_d \sim 3.6$ GeV and can be fulfilled at GSI-SIS where the maximum deuteron kinetic energy T_d^{max} is 4 GeV.

We now estimate the reaction cross section by using the nuclear response function $S(E)$:

$$\left(\frac{d^2\sigma}{d\Omega dE}\right)_{A(d,^3He)_\eta(A-1)} = \left(\frac{d\sigma}{d\Omega}\right)^{lab}_{p(d,^3He)\eta} \times \sum_{l_\eta, j_n, J} S(E) \tag{6}$$

where $\left(\frac{d\sigma}{d\Omega}\right)^{lab}_{p(d,^3He)\eta}$ is the elementary cross section in the laboratory frame. A comprehensive and consistent approach to calculate the response function

$S(E)$ for a system with a large imaginary potential was formulated by Morimatsu and Yazaki[19]. This method uses the Green function $G(E;\vec{r},\vec{r}')$ defined as

$$G(E;\vec{r},\vec{r}') = < p^{-1}|\phi_\eta(\vec{r})\frac{1}{E-H_\eta+i\epsilon}\phi_\eta^\dagger(\vec{r}')|p^{-1}>, \tag{7}$$

where $\phi_\eta^\dagger$ is the η creation operator and $|p^{-1}>$ is a proton hole state. The Hamiltonian H_η contains the $\eta-$nucleus optical potential. Since we used energy-independent local potentials in the present calculation, we can obtain a simple expression for the Green function as

$$G(E;\vec{r},\vec{r}') = \sum_{l_\eta,m_\eta} Y^*_{l_\eta,m_\eta}(\hat{r})Y_{l_\eta,m_\eta}(\hat{r}')G_{l_\eta}(E;r,r') \tag{8}$$

$$G_{l_\eta}(E;r,r') = -2\mu k u_{l_\eta}(k,r_<)v^{(+)}_{l_\eta}(k,r_>), \tag{9}$$

where u_{l_η} and $v^{(+)}_{l_\eta}$ respectively are the radial part of the regular and outgoing solutions of equation of motion. Using the Green function, the response can be calculated as

$$S(E) = -\frac{1}{\pi}Im\sum_{M,m_s}\int d^3r d\sigma d^3r' d\sigma' f^\dagger(\vec{r},\sigma)G(E;r,r')f(\vec{r'},\sigma'). \tag{10}$$

We define $f(\vec{r},\sigma)$ as

$$f(\vec{r},\sigma) = \chi_f^*(\vec{r})\xi^*_{\frac{1}{2},m_s}(\sigma)[Y^*_{l_\eta}(\hat{r})\otimes\psi_{j_p}(\vec{r},\sigma)]_{JM}\chi_i(\vec{r}), \tag{11}$$

where χ_i and χ_f respectively denote the projectile and the ejectile distorted waves, ψ is the proton hole wavefunction and ξ is the spin wavefunction introduced to count possible spin directions of the proton in the target nucleus. The numerical values of $S(E)$ were evaluated by using the eikonal approximation as in the case of deeply-bound pionic atoms [20].

The elementary cross section for η production which appears in Eq.(6) can be inferred from the energy dependence of the p(d,^{3}He)η cross section measured at SATURNE[21] in the d(p,^{3}He) reaction. At $T_p = 1.75$ GeV (this proton kinetic energy corresponds to the recoilless η production in the p(d,^{3}He)η reaction), the c.m. cross section $(d\sigma/d\Omega)_{cm}$ is 3 nb/sr. This can be translated to the $d+p$ laboratory-frame cross section via

$$\frac{d\sigma}{d\Omega}_{lab} = \left(\frac{p_{lab}(^3\mathrm{He})}{p_{cm}(^3\mathrm{He})}\right)^2\frac{d\sigma}{d\Omega}_{cm}, \tag{12}$$

and the approximate elementary cross section was deduced to be 150 nb/sr.

In Fig. 2, we show the calculated spectra using the Green function method described above. The results are shown for the ^{7}Li target (left panel) and for the ^{12}C target (right panel), for different potential parameters. The top and middle figures respectively correspond to the ηN scattering lengths of Eq.(2) ($V(r) = -(86 + 32i)\rho(r)/\rho_0$ MeV) and Eq.(4) ($V(r) = -(62 + 30i)\rho(r)/\rho_0$ MeV). The bottom figures are for the potential with no binding, $V(r) = -30i\rho(r)/\rho_0$ MeV.

In solid lines, the expected double-differential forward ($0°$) cross sections are shown. The dashed and dash-dotted lines respectively show the contributions from the $(p_{3/2})_p^{-1} \otimes (2p)_\eta$ and the $(s_{1/2})_p^{-1} \otimes (1s)_\eta$ substitutional configurations. These two configurations contribute dominantly to the Q-value spectra, although we in fact calculated contributions from other partial waves (up to $l = 6$) and confirmed that there are no significant contributions from partial waves beyond $l = 6$.

The vertical lines indicate the η production thresholds; for the ^{7}Li case, the threshold is at $Q_0 = -552$ MeV while it is at $Q_0 = -558$ MeV for the ^{12}C case. The η binding energy B_η can be deduced from the reaction Q value as (for the sake of simplicity we ignore the nuclear recoil energy, which is small near the recoilless condition):

$$Q - Q_0 = B_\eta - (S_p(j_p) - S_p(p_{3/2})), \tag{13}$$

where $(S_p(j_p) - S_p(p_{3/2}))$ is the proton hole energy measured from the ground state of the residual nuclei. Hence, for the η states coupled to the $(s_{1/2})_p^{-1}$ configuration, the $(\mathrm{s}_{1/2})_\mathrm{p}^{-1} - (\mathrm{p}_{3/2})_\mathrm{p}^{-1}$ energy differences (14 MeV for ^{7}Li and 18 MeV for ^{12}C) taken from ref. [22] was added when calculating these spectra.

Note that the ground state of the $\eta-$nucleus system for these light $p-$shell targets would have the $(p_{3/2})_p^{-1} \otimes (1s)_\eta$ configuration, but this component does not contribute to the Q-value spectra near the recoilless condition. Instead, the dominant contribution comes from the $(p_{3/2})_p^{-1} \otimes (2p)_\eta$ configuration, and we can determine the $\eta-$nucleus potential from the location of the $2p$ peak. This $(p_{3/2})_p^{-1} \otimes (2p)_\eta$ component is more dominant in the ^{12}C case because there are four $p_{3/2}$ protons in a ^{12}C nucleus as compared to only one in a ^{7}Li nucleus.

In Fig.3, we show the calculated spectrum for a heavier target, ^{40}Ca. The potential strength corresponds to the scattering length in eq. (4). Due to the recoilless condition, dominant contributions come from the substitutional states. However, as can be seen in the figure, several proton-hole states contribute to a broad maximum in the Q value spectrum which makes the interpretation

difficult. We therefore conclude that light nuclei like those in the p-shell region are most suitable to search for bound nuclear states of η mesons.

In order to generate realistic Q-value spectra we also have to include background contributions from other reactions, which we will discuss in the following.

We first note that the background due to ^{3}He formation without meson production (such as due to coalescence) must be negligible. Composite particle production with a few GeV protons incident on nuclear targets was studied by Tokushuku *et al.* [23] at KEK. By extrapolating their results on the deuteron spectra in the Al(p,d) reaction at $T_p = 3$ GeV to $p_d \sim 4$ GeV/c, we found the cross section to be around 10^{-9}[nb/(MeV/c)sr], which is negligibly small.

The continuum background for η production was estimated by using the data of Berthet *et al.* [21]. By relating the number of events for η production as shown in figure 1(b) of Ref. [21] to the tabulated c.m. cross section, we estimated the c.m. continuum background level to be ~ 0.09nb/sr/MeV at $T_p = 2$ GeV ($T_d = 4$ GeV). This corresponds to $d^2\sigma/dEd\Omega_{lab} \sim 4.5$ nb/sr/MeV in the (d,^{3}He) laboratory frame.

The d(p,^{3}He)$\pi^+\pi^-$ data near the η threshold by Mayer *et al.*[24] show that the continuum background due to $\pi^+\pi^-$ production is nearly flat across the η production threshold. We therefore ignored the possible Q-value dependence of the continuum background.

In order to evaluate the continuum background for the case of nuclear targets, we need to calculate the distortion effects of the deuteron and the ^{3}He in the target nucleus. For this purpose, we summed up the effective numbers for all final state configurations of proton-hole and mesonic states. The calculated effective proton numbers had negligible energy dependence. We further assumed that the contributions of target protons and neutrons to the background is identical, and hence multiplied the calculated effective number by a factor A/Z. This total effective number is expected to be a good estimation of the distortion effects to the projectile and the ejectile. And this is also expected to be consistent with the estimation of signal cross sections. The effective nucleon number contributing to the background was calculated, and was used to estimate the constant background level as:

$$\begin{aligned} N_{\rm eff} &= 0.253 \times 7/3 \\ &\rightarrow \left(\frac{d\sigma}{dEd\Omega}\right)_{\rm background} = 4.5 \times 0.253 \times 7/3 = 2.7\text{nb/sr/MeV} \quad \text{for}^7\text{Li} \\ N_{\rm eff} &= 0.373 \times 12/6 \end{aligned}$$

$$\rightarrow \left(\frac{d\sigma}{dEd\Omega}\right)_{\text{background}} = 4.5 \times 0.373 \times 12/6 = 3.4\text{nb/sr/MeV} \quad \text{for}^{12}\text{C}.$$

In Fig.4, we show expected Q-value spectra for the ^{7}Li case assuming 100 hours of beam time at GSI, using the FRS as ^{3}He spectrometer. As shown, we expect the peaks to be clearly visible above background, and the spectra are sensitive enough to differentiate between various $\eta-$nucleus potential parameters. The experimental setup will be similar to the one used for the study of deeply-bound pionic atoms. For the estimate we used a target thickness of 1g/cm^2, a deuteron beam intensity of 3×10^{10}/sec at 3.5 GeV incident energy, and $\Omega = 2.5 \times 10^{-3}$sr for the FRS acceptance; all these parameters are achievable at GSI.

Here, we would like to mention that the (d,^{3}He) reaction is also well-suited for the production of ω-mesic nuclei. In Fig.5, we show calculated spectra for ω production in the (d,^{3}He) reaction on ^{7}Li at $T_d = 3.8$ GeV (also possible at GSI), in which we compare three different ω-nucleus optical potentials. At this incident energy, however, the recoilless condition is not satisfied, and we hence find that the contributions from substitutional states are not dominant, and that the quasi-free process makes a large contribution in the unbound region. Although the identification of bound states appears to be difficult, the effect of an attractive ω-nucleus potential is noticeable in the bound region of the Q value spectrum.

In order to see the effect of the recoil free condition for ω production we show in Fig.6 the calculated Q value spectrum at 10 GeV incident deuteron energy. We assumed the elementary ω production cross section to be 450 nb/sr. In this case, as in the η-production spectrum at $T_d = 3.8$ GeV, the dominant contributions result from substitutional states. With less configurations contributing the ω-nucleus optical potential may be deduced from the spectral shape more directly.

One should note that the (d,^{3}He) reaction is the nucleon pickup reaction, allowing for recoil free η and ω production, with the lightest projectile and ejectile nuclei. The (p,d) reaction which may also satisfy the recoil free condition at appropriate incident energy, however does not allow to separate the ejectiles from the beam particles in a magnetic spectrometer due to the same magnetic rigidity in the case of vanishing momentum transfer.

In conclusion, we find that the proposed recoilless (d,^{3}He) reaction is a promising tool to study the $\eta-$nucleus system, and we should be able to determine the $\eta-$nucleus potential (and the possible η mass shift in nuclei) from the Q-value spectra. In principle, this method can be extended to study the behavior of other mesons such as ω in nuclei, although there is at present no

facility in the world where one can study ω production near the recoilless condition ($T_d \sim 10$ GeV is required). The proposed method is complementary to studies of vector mesons in nuclear matter by analysing their invariant mass spectrum in the dilepton decay channel, such as $\omega \to e^+e^-$. A proposed experimental study of η and ω production in the (d,^{3}He) reaction at low mometum transfer [10] was recently approved at GSI.

The authors would like to thank H. Toki, T.-S. H. Lee, K. Itahashi, H. Gilg, F. Klingl, T. Waas, W. Weise, P. Kienle and T. Yamazaki for helpful discussions. This work is supported in part by the Grant-in-Aid for Scientific Research, Monbusho, Japan.

References

[1] S. Klimt, M. Lutz, U. Vogl, and W. Weise, Nucl. Phys. A516(1990)429

[2] See, for instance, T. Hatsuda and T. Kunihiro, Phys. Rep. 247(1994)241; G. E. Brown and M. Rho, Phys. Rep. 269(1996)333

[3] Q. Haider and L. C. Liu; Phys. Lett. B172(1986)257, Phys. Rev. C34(1986)1845

[4] R. E. Chrien et al., Phys. Rev. Lett 60(1988)2595

[5] J. Berger et al., Phys. Rev. Lett. 61(1988)919

[6] C. Wilkin, Phys. Rev. C47 (1993) R938

[7] N. Willis et al., Phys. Lett B406(1997)14

[8] H. C. Chiang, E. Oset, and L. C. Liu, Phys. Rev. C44(1991)738

[9] S. A. Rakityansky et al., Phys. Rev. C53 (1996)R2043

[10] R. S. Hayano, A. Gillitzer et al., GSI proposal S214 (1997).

[11] S. Hirenzaki, H. Toki, T. Yamazaki, Phys. Rev. C44(1991)2472

[12] T. Yamazaki et al., Z. Phys. A355 (1996) 219

[13] T. Waas, R. Brockmann, and W. Weise, Phys. Lett. B405(1997)215.

[14] T. Yamazaki et al., Phys. Lett B418 (1998) 246.

[15] T. Hatsuda and S. H. Lee, Phys. Rev. C46(1992)R34

[16] M. Batinić *et al.* nucl-th/9703023. This is an update to their original work published in Phys. Rev. C51 (1995) 2310 and its erratum, Phys. Rev. C57 (1998) 1004.

[17] A.M. Green, S. Wycech, Phys. Rev. C55 (1997) R2167.

[18] N. Kaiser, T. Waas, W. Weise, Nucl. Phys. A612 (1996) 297.

[19] O. Morimatsu and K. Yazaki, Nucl. Phys. A435 (1985) 727; Nucl. Phys. A483 (1988) 493.

[20] H. Toki, S. Hirenzaki and T. Yamazaki, Nucl. Phys. A530 (1991) 679.

[21] P. Berthet *et al.*, Nucl. Phys. A443 (1985) 589.

[22] S.L. Belostotskii *et al.*, Sov. J. Nucl. Phys. 41 (1985) 903.

[23] K. Tokushuku, *et al.*, Phys. Lett. 235B (1990) 245.

[24] B. Mayer *et al.*, Phys. Rev. C53 (1996) 2068.

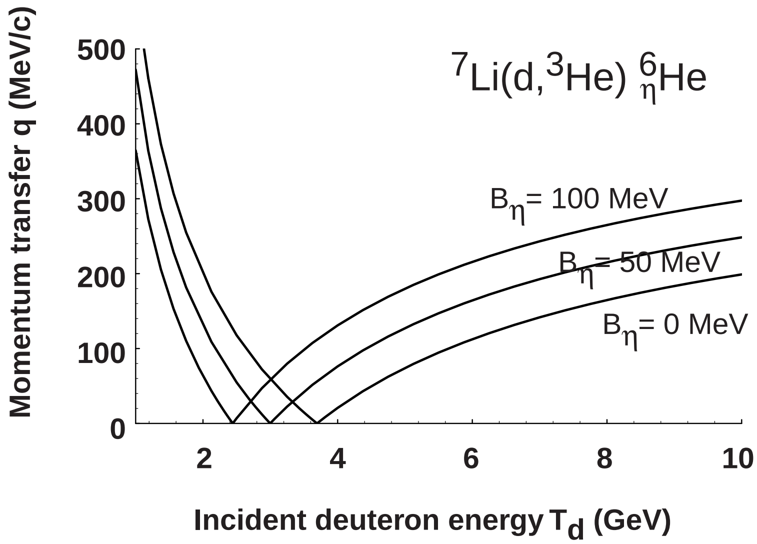

Fig. 1. *The momentum transfer q vs. incident deuteron kinetic energy T_d in the $^7Li(d,^3He)^6_\eta He$ reaction. The three curves respectively correspond to η binding energies of 100, 50 and 0 MeV, as indicated*

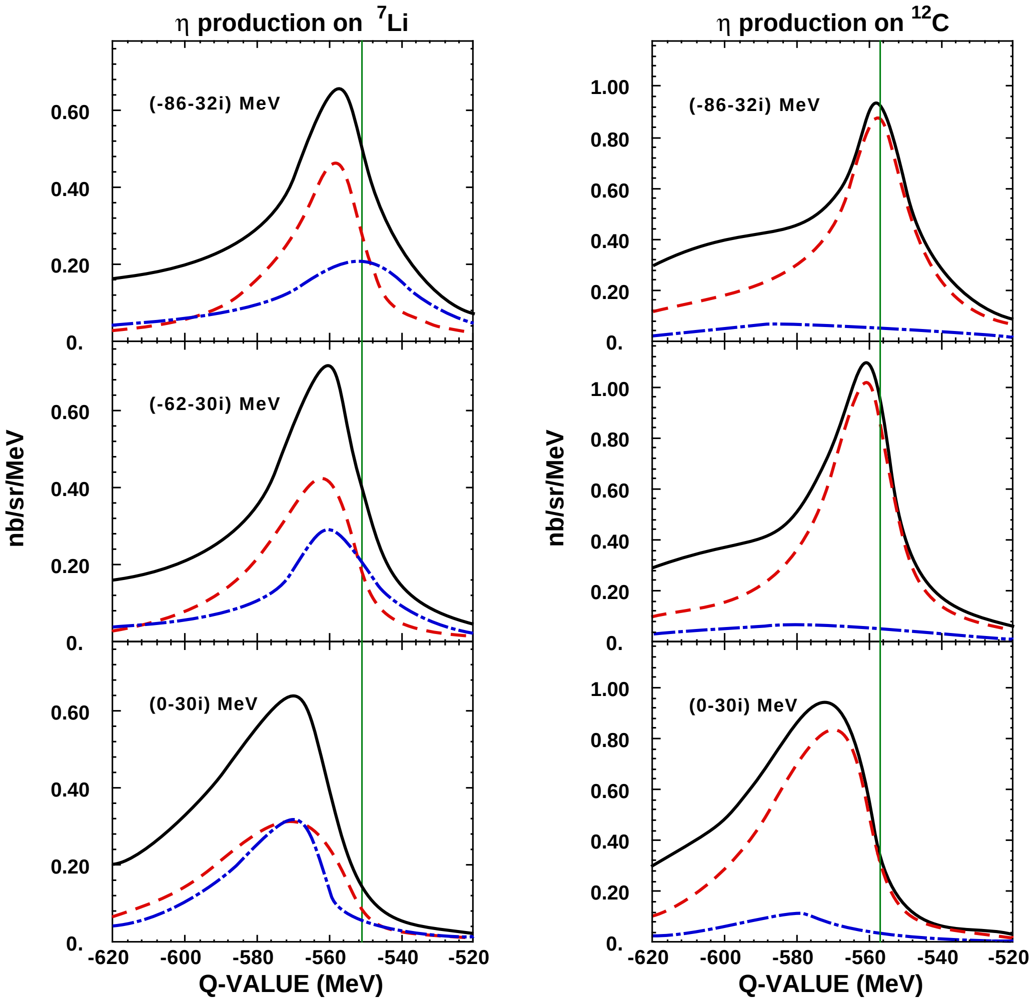

Fig. 2. *The calculated* η *production spectra for the* ^{7}*Li(d,*^{3}*He) reaction (left) and for the* ^{12}*C(d,*^{3}*He) reaction (right) at* $T_d = 3.5$ *GeV, for three different* η*-nucleus optical potential parameters; (top)* $V = -(86 + 32i)\rho/\rho_0$ *MeV, (middle)* $V = -(62 + 30i)\rho/\rho_0$ *MeV, (bottom)* $V = -30i\rho/\rho_0$ *MeV. The vertical lines indicate the* η *production threshold Q-value (*$Q_0 = -552$ *MeV for the Li case and -558 MeV for the C case). In each figure, the contribution from the* $(0p_{3/2})_p^{-1} \otimes p_\eta$ *is shown in a dashed curve, the* $(0s_{1/2})_p^{-1} \otimes s_\eta$ *contribution is shown in a dash-dotted curve, and the solid curve is the sum of* η*-partial waves up to* $l = 6$*. The continuum background contributions are estimated to be about 2.7 nb/sr/MeV for the* ^{7}*Li target and 3.4 nb/sr/MeV for the* ^{12}*C target (see text).*

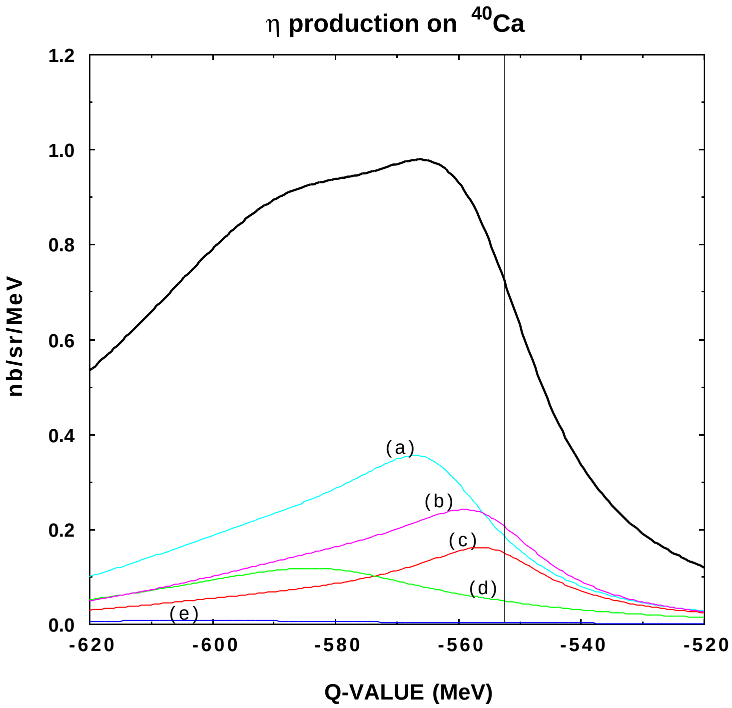

Fig. 3. *The calculated η production spectrum for the ^{40}Ca(d,^{3}He) reaction at $T_d = 3.5$ GeV, for $V = -(62 + 30i)\rho/\rho_0$ MeV. The labelled curves denote contributions from the following configurations: a) $[(1d_{5/2})_p^{-1} \otimes d_\eta]$, b) $[(1d_{3/2})_p^{-1} \otimes d_\eta]$, c) $[(2s)_p^{-1} \otimes s_\eta]$, d) $[(1p)_p^{-1} \otimes p_\eta]$ and e) $(1s)_p^{-1} \otimes s_\eta$.*

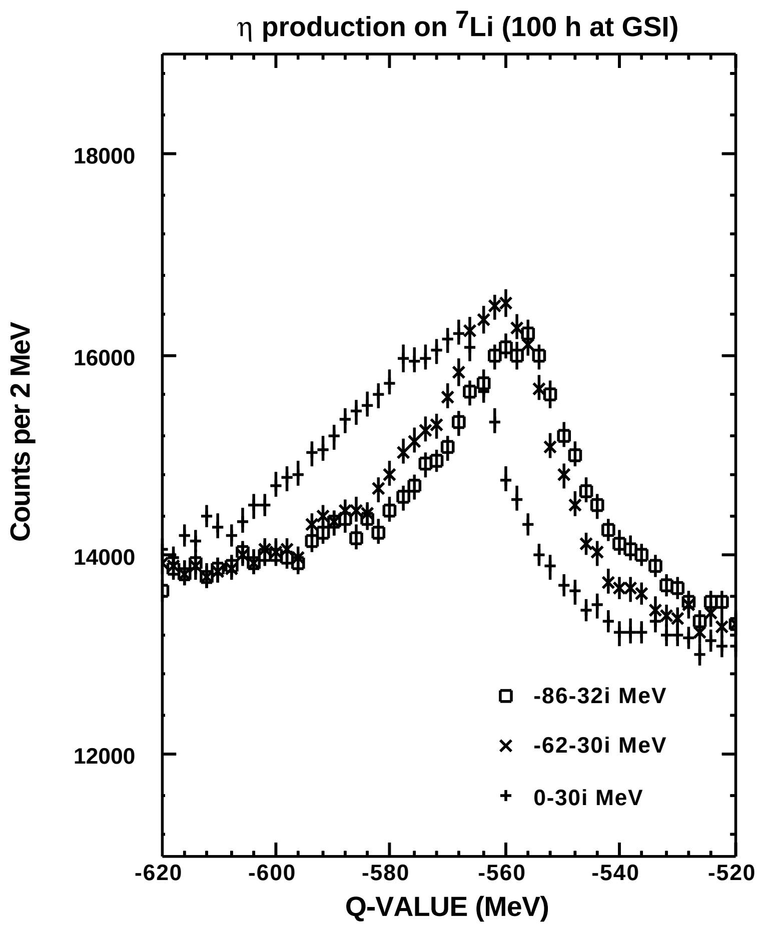

Fig. 4. *Expected Q value spectrum for the* ^{7}*Li(d,*^{3}*He) reaction near the* η *production threshold for 100 hours of running at GSI (see text for assumptions of the experimental conditions).*

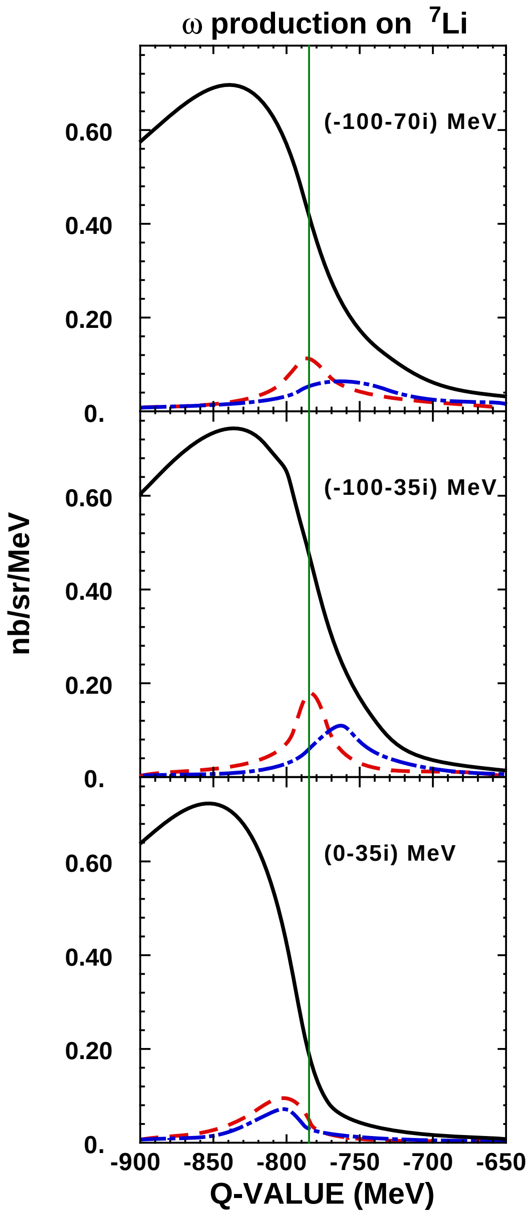

Fig. 5. *The calculated ω production spectra for the ^{7}Li(d,^{3}He) reaction at $T_d = 3.8$ GeV, for three different ω-nucleus optical potential parameters; (top) $V = -(100 + 70i)\rho/\rho_0$ MeV, (middle) $V = -(100 + 35i)\rho/\rho_0$ MeV, (bottom) $V = -35i\rho/\rho_0$ MeV. The vertical lines indicate the ω production threshold of $Q_0 = -787$ MeV. In each figure, the contribution from the $(0p_{3/2})_p^{-1} \otimes p_\omega$ is shown in a dashed curve, the $(0s_{1/2})_p^{-1} \otimes s_\omega$ contribution is shown in a dash-dotted curve, and the solid curve is the sum of partial waves up to $l = 6$. The continuum background contributions are estimated to be about 7.7 nb/sr/MeV.*

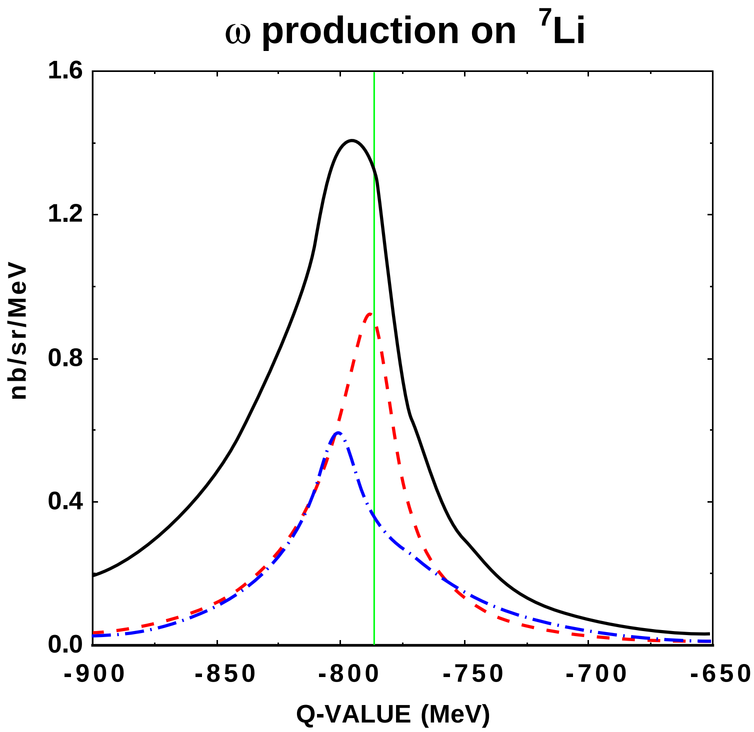

Fig. 6. *The calculated ω production spectrum for the ^{7}Li(d,^{3}He) reaction at $T_d = 10$ GeV. The elementary cross section was assumed to be 450 nb/sr. The contribution from the $(0p_{3/2})_p^{-1} \otimes p_\eta$ is shown in a dashed curve and the $(0s_{1/2})_p^{-1} \otimes s_\eta$ contribution is shown in a dash-dotted curve. The solid curve is the sum of $\omega-$partial waves up to $l = 6$.*

Table 1
A-dependence of the η-nucleus binding energies and widths. We use $a_{\eta N} = 0.717 + 0.263i$ $[fm]$ as η-N scattering length.

A	$\ell = 0$		$\ell = 1$		$\ell = 2$		$\ell = 3$	
	B.E.(MeV)	Γ (MeV)	B.E.(MeV)	Γ (MeV)	B.E.(MeV)	Γ (MeV)	B.E.(MeV)	Γ (MeV)
6	17.4	33.5						
11	35.3	48.8						
15	44.4	55.5	9.61	35.9				
19	50.8	59.9	17.7	43.0				
31	62.0	66.3	34.1	55.2	5.87	40.2		
	4.36	34.4						
39	66.4	68.2	40.8	59.1	15.0	48.0		
	11.8	44.5						
64	74.3	71.8	53.3	63.4	31.4	58.8	10.6	52.0
	25.8	58.2						
88	77.6	73.2	61.0	66.8	40.1	59.4	21.4	60.1
	33.3	56.7						
132	80.5	73.2	67.9	70.4	52.6	64.2	32.5	56.9
	47.4	61.4	20.9	53.1				
207	83.0	73.5	72.4	70.1	62.1	69.8	49.5	64.8
	58.5	70.6	43.4	62.1	15.7	39.6		
	11.4	30.4						

Table 2
A-dependence of the η-nucleus binding energies and widths. We use $a_{\eta N} = 0.20 + 0.26i$ $[fm]$ as η-N scattering length.

A	$\ell = 0$		$\ell = 1$		$\ell = 2$		$\ell = 3$	
	B.E.(MeV)	Γ (MeV)	B.E.(MeV)	Γ (MeV)	B.E.(MeV)	Γ (MeV)	B.E.(MeV)	Γ (MeV)
31								
39	5.25	51.9						
64	9.41	57.2						
88	11.7	59.0						
132	14.2	60.6						
207	16.2	61.8	9.09	57.2				